# Microstrip Conductor Loss Models for Electromagnetic Analysis

James C. Rautio, *Fellow, IEEE,* and Veysel Demir, *Student Member, IEEE,*

***Abstract*—This paper describes and rigorously validates single- and multiple-layer models of microstrip conductor loss appropriate for high-accuracy application in electromagnetic analysis software. The models are validated by comparison with measurement and by comparison with converged results. It is shown that in some cases an extremely small cell size is needed in order to achieve convergence. Several effects that make a significant contribution to loss and are not modeled by the classic square root of frequency loss model are investigated including dispersion and current on the side of transmission lines. Finally, the counterintuitive result that there is an optimum metal thickness for minimum planar conductor loss is explored.**

***Index Terms*—Conductivity, dispersion, electromagnetic, high frequency, loss, microstrip, microwave, resistance, skin effect, stripline, surface impedance.**

## I. Background

IT IS well known that high-frequency current in a planar conductor (Figs. 1 and 2) decreases exponentially with penetration into the conductor, falling to $1/e$ of its surface value at one skin depth

$$\delta = \sqrt{\frac{2}{\omega\mu\sigma}} \tag{1}$$

where $\delta$ is skin depth, $\mu$ is conductor magnetic permeability, $\sigma$ is bulk conductivity, and $\omega$ is radian frequency. The current density as a plane wave penetrates into an infinitely thick conductor (with the $z$ axis perpendicular to the conductor surface) is

$$J(z) = J_0 e^{-z/\delta}\big(\cos(z/\delta) - j\sin(z/\delta)\big) \tag{2}$$

where $J_0$ is the current density at surface of conductor, perpendicular to the $z$ axis.

The complete analysis of an actual finite thickness conductor with finite bulk conductivity in electromagnetic analysis software can be numerically intensive. Instead, a thick conductor is usually modeled as an infinitely thin conductor with an equivalent surface impedance $Z_S$ equal to the characteristic impedance $Z_{0M}$ of a plane wave propagating along the $z$ axis into the conductor

$$Z_S = Z_{0M} = \sqrt{\frac{j\omega\mu}{\sigma}} = (1+j)\sqrt{\frac{\omega\mu}{2\sigma}}. \tag{3}$$

Manuscript received May 3, 2002; revised October 1, 2002.

The authors are with Sonnet Software Inc., Liverpool, NY 13088 USA (e-mail: rautio@sonnetusa.com).

Digital Object Identifier 10.1109/TMTT.2003.808693

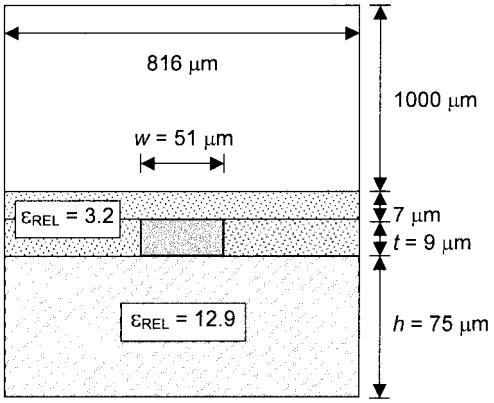


Fig. 1. Transmission-line geometry used for validation. The substrate is GaAs with polyimide passivation. In the actual line, the polyimide is 7 $\mu$m thick everywhere. The loss tangent of the polyimide is 0.005, and the GaAs is 0.0005. The line is 6.888 mm long. Drawing not to scale.

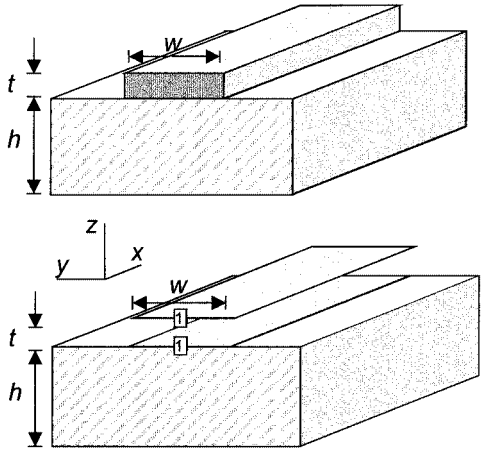


Fig. 2. Actual transmission line (above) is modeled by the two-layer model (below). Note that both sheets at a port location carry the same port number.

This equivalent surface impedance is correct only for good conductors much thicker than the skin depth. It is also correct only for current flowing on one side of a conductor.

In [1], it is shown that the equivalent surface impedance of a conductor of thickness $t$ is

$$Z_S = -jZ_{0M}\cot(kt) \tag{4}$$

where

$$k = \sqrt{-j\omega\mu\sigma} = (1-j)\sqrt{\frac{(\omega\mu\sigma)}{2}} = (1-j)\frac{1}{\delta}.$$

The expression for surface impedance in [2] is a close approximation of this result. In [3] and [4], a similar equation is pre-

sented. The bibliography of [3] is especially useful for reviewing the historical development of the skin effect. Note that (4) is the input impedance of a transmission line with length equal to the metal thickness $t$, using the propagation velocity and impedance of a plane wave propagating in the metal. This transmission line is assumed to be terminated in an open circuit. Multiple layers of differing metals use a cascade of appropriate transmission lines [5].

This equation can also be written as

$$Z_S = (1-j)R_{\rm RF}\sqrt{f}\cot\left((1-j)R_{\rm RF}\sqrt{f}\frac{1}{R_{\rm DC}}\right) \quad (5)$$

where

$$R_{\rm DC} = \frac{1}{\sigma t} \quad (6)$$

$$R_{\rm RF} = \sqrt{\frac{\pi\mu}{\sigma}}$$

and

$$f = \text{frequency}. \quad (7)$$

By expanding (5) into its exponential form, it can be seen that $Z_S = R_{\rm DC}$ at low frequency and $Z_S = Z_{0M} = (1+j)R_{\rm RF}\sqrt{f}$ at high frequency. This is the form used in the Sonnet analysis [6].

## II. Transition Frequencies

As detailed in [2] and summarized here, there are three frequency ranges, each range exhibiting a distinct loss characteristic.

1) At low frequencies, skin depth is large compared to thickness and current is effectively evenly distributed through out the conductor volume. A conductor is considered to be electrically thin in this frequency region. The edge singularity is of no consequence and loss is constant with frequency.
2) When the resistance per unit length $R$ equals the inductive reactance per unit length $\omega L$, the edge singularity begins to form. Loss increases as the edge singularity emerges from the uniform low-frequency current distribution. Once it has completely emerged, except for the effect of dispersion, loss is once more constant with frequency. This transition starts at

$$f_{c1} = R/2\pi L \quad (8)$$

where $R$ is the resistance per unit length $(=1/(\sigma wt)$, $w$ is width, and $t$ is thickness) and $L$ is the inductance per unit length $(=Z_0/v$, $Z_0$ is the characteristic impedance, and $v$ is the velocity of propagation). While this expression for the first transition frequency seems to be intuitively reasonable, it should be carefully noted that it is based purely on empirical observation.
3) When the conductor is thick compared to skin depth, loss increases because current is increasingly confined to the surface of the conductor. It is in this region in which the classic square root of frequency behavior can occur. The transition frequency is selected to be where the conductor is two skin depths thick (current is assumed flowing on both top and bottom surfaces) as follows:

$$f_{c2} = \frac{4}{\pi\mu\sigma t^2}. \quad (9)$$

As pointed out in [2], while $f_{c1}$ is usually lower than $f_{c2}$, in some situations the transition frequencies can actually reverse order. These transition frequencies correspond to and are dimensionally the same as transition frequencies proposed in [7], where microstrip loss is modeled by interpolation between solutions obtained for each region, rather than by application of (4). The transition frequencies used in [7] are also used in [8] with some modification; however, the region between the two transition frequencies is viewed as a single transition with a beginning and an end. Microstrip loss in [8] for this region is modeled by fitting to mode-matching results.

## III. The $N$-Layer Model

Using Sonnet [6], we devised a rigorous multilayer model to use in the validation of more efficient loss models (the two-layer model is shown in Fig. 2). The number of layers is selected so that each layer, of thickness $t/n$, is thin compared to skin depth. The entire thick conductor is modeled as a group of $n$ sheets, each separated by a distance of $t/(n-1)$, with a surface impedance of

$$Z_S = n/\sigma t = nR_{\rm DC}. \quad (10)$$

This is the low-frequency (electrically thin) case of (5). The $n$ layers connected in parallel yield a total resistance of $1/\sigma t$ at low frequency where the current divides evenly between all $n$ layers and edge singularity is of no consequence. At high frequencies, current flows preferentially on the outer layers and on the outer edges according to the solution of Maxwell's equations. This causes the total transmission-line resistance to increase with frequency. For this model, all the frequency variation of resistance is due to the solution of Maxwell's equations. There is no *a priori* assumption as to what form this frequency variation should take.

For this model, as long as each individual layer is thin compared to skin depth, the result should be as accurate as the electromagnetic analysis used to solve the $n$-layer system. In the case of Sonnet, the electromagnetic analysis has been validated to be asymptotically exact to better than 0.1% [9].

Fig. 3 shows the 81-layer model results compared to measurement. The transmission line (Fig. 1) is 6.888 mm long. Since the line is uniform, only $1/32$ of the entire length is analyzed. The fully deembedded result is then cascaded with itself 32 times for the final result. The conductivity of $3.45\times10^7$ S/m as measured by a precision Ohm-meter, and the measured $S$-parameters are an average of measurements from four separate identical lines. Full details are provided in [2], except that ground loss is now included assuming the same loss parameters as the top-side metal.

Results are presented for the 81-layer model (each layer just over 0.1 $\mu$m thick) for various cell widths. The result for the line subsectioned two cells wide is equivalent to assuming a uniform current distribution, i.e., there is no loss due to an edge singularity. Results for the line subsectioned 64 cells wide and 128 cells wide are identical to within $\pm0.02$ dB. A 41-layer model

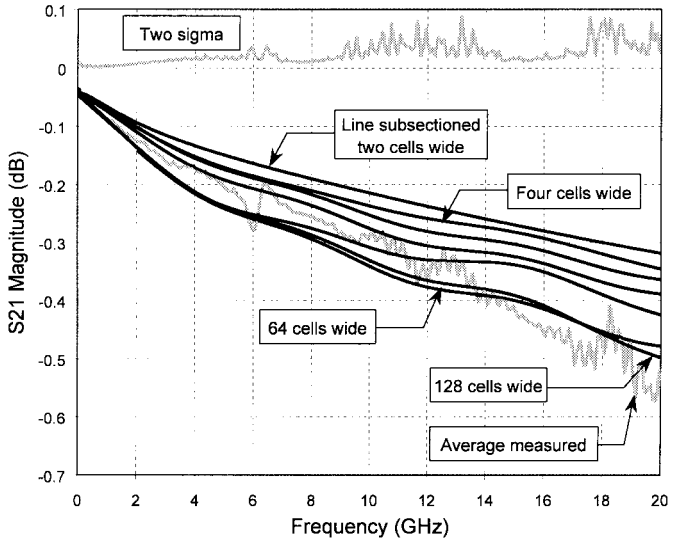


Fig. 3. To check convergence of the 81-layer model, cell width used in the electromagnetic analysis is decreased, increasing the number of cells across the width of the microstrip line of Fig. 1. The number of cells into which the line width is divided is doubled for each successive curve (not all labeled). Line geometry is shown in Fig. 1.

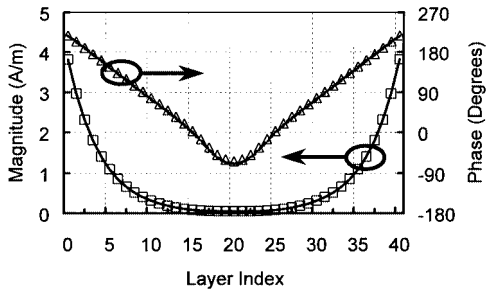


Fig. 4. To further validate the $n$-layer model, the current on each layer (solid lines) as calculated by the 41-layer model of a stripline is compared with expected current (see (2), symbols). Stripline geometry: $w = 400\ \mu$m, $t = 8.6\ \mu$m, $\sigma = 3.45 \times 10^7, \varepsilon_r = 1.0$, ground plane spacing $= 18.6\ \mu$m, analyzed at 10 GHz with a 20 $\mu$m $\times$ 20 $\mu$m cell size.

was also evaluated with results for the line 128 cells wide also within $\pm 0.02$ dB of the 81-layer model at all frequencies. The converged results are generally within two sigma of the measured data except around the measurement resonance at 6 GHz.

All analyses presented in this paper are performed using the Sonnet ABS interpolation [10], requiring analyses from three to five frequencies to cover 0.05–20.05 GHz to an interpolation error of less than $\pm 0.0003$ dB. Analysis times for the 81-layer model range from 3 min to 8 h per frequency on a 1.3-GHz Pentium. All coupling between all 81 layers is calculated to full numerical precision.

To further validate the $n$-layer model, Fig. 4 shows how current magnitude and phase vary with depth into the conductor for a stripline as calculated by Sonnet. Data markers from (2) are modified to include current flowing on both sides of the conductor (by adding a mirror image of (2) to itself).

## IV. Two-Layer Model

The two-layer model divides the volume of the conductor into two equal layers. It is modeled with two infinitely thin sheets,

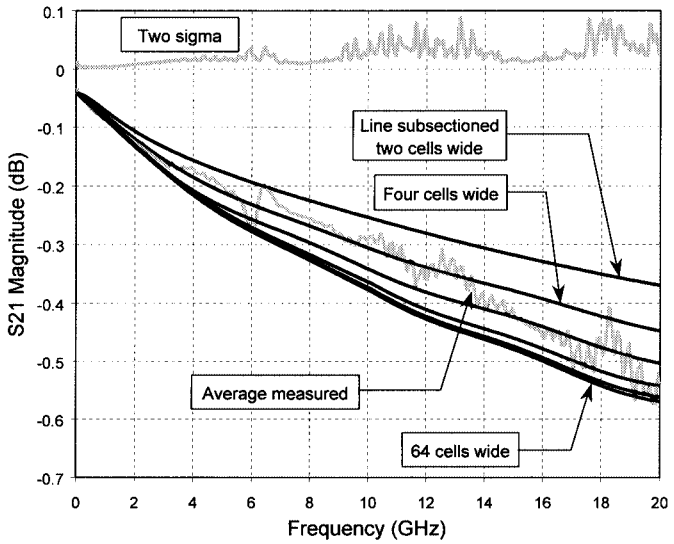


Fig. 5. Convergence occurs more rapidly for the two-layer model, however, high-frequency loss converges 0.07 dB higher than for the 81-layer model. Microstrip geometry is shown in Fig. 1.

one at the top surface of the actual conductor and the other at the bottom (Fig. 2). In contrast to the $n$-layer model, each sheet is assumed to have the frequency-dependent surface impedance (4) using a thickness of one half the total metal thickness. When using (5), one need only multiply $R_{\rm DC}$ by 2.

Fig. 5 shows the two-layer model convergence for the same microstrip line of Fig. 2. Note that the 32-cell-wide result is within 0.02 dB of the 64-cell-wide result. In addition, the convergence is smooth so, at least in this case, Richardson extrapolation [11] can be used to advantage. Analysis times range from under 1 s to 34 s per frequency, much faster than the 81-layer model.

Note that the two-layer model at high frequency has converged to 0.07 dB (about 15%) more loss than the converged 81-layer model (Fig. 3). As discussed later, we suggest that this is due to current flowing on the lateral sides of the microstrip line. Such current is not included in the two-layer model, but is included in the 81-layer model. As such, the two-layer model overestimates loss when the microstrip line is more than a few skin depths thick. This microstrip line is 15 skin depths thick at 20 GHz.

Side current can also account for the slower convergence of the 81-layer model. Since current flowing on the side of the actual thick line is concentrated within one skin depth of the surface, the cell width of most of the 81 layers must be on the order of the skin depth for accurate modeling. This is not achieved for the 81-layer model until the width is subdivided into 128 cells, yielding a cell width of just under 0.4 $\mu$m. Skin depth is 0.6 $\mu$m at 20 GHz. The 32-cell-wide curve in Fig. 3 is especially interesting because the side current appears to be well modeled below 10 GHz, but not above 12 GHz. If one were to model this thick line to this same accuracy using a volume meshing analysis, a similar mesh size (81 $\times$ 128 cells across the cross section of the line) would be required.

Fig. 6 shows that the frequency-dependent two-layer model is the limit to which the multilayer model (with frequency-independent surface resistance) converges. The line is 400 $\mu$m

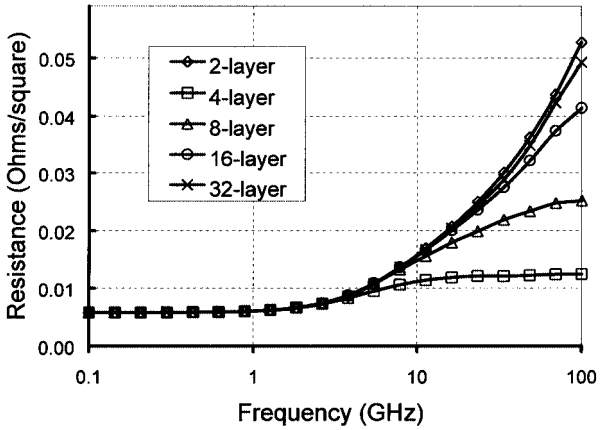


Fig. 6. Convergence of the $n$-layer model to the two-layer model is shown for a 400-$\mu$m-wide stripline. All the models except the two-layer use frequency-independent loss. This demonstrates that the two-layer model with frequency-dependent surface impedance is the limit to which the $n$-layer model converges when side current is not a factor. Stripline geometry: $w = 400\ \mu$m, $t = 4.2843\ \mu$m, $\sigma = 3.45 \times 10^7, \varepsilon_r = 1.0$, ground plane spacing $= 24.2843\ \mu$m, $(W \times L)\ 25\ \mu\text{m} \times 5\ \mu$m cell size.

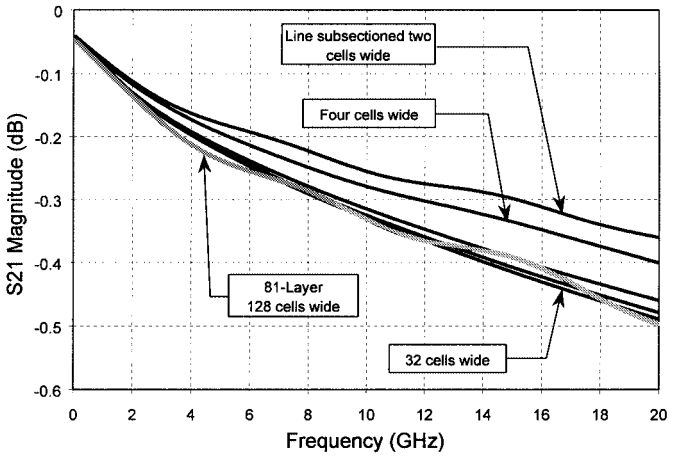


Fig. 7. Convergence occurs even more rapidly for the one-layer model, and the result is nearly identical to the 81-layer 128-cell-wide result. Microstrip geometry is shown in Fig. 1.

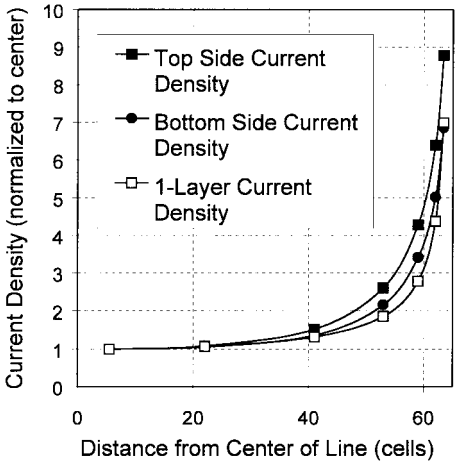


Fig. 8. Current density on the top and bottom surfaces of the two-layer model is compared with the current density of the one-layer model. Data are taken at the center of each subsection with a smooth line drawn between. The actual current distribution used in the analysis is piece-wise constant. Microstrip geometry is shown in Fig. 1. Analysis frequency is 20 GHz.

wide and just over 4 $\mu$m thick with a ground plane spacing of 24.28 $\mu$m, so side current is substantially reduced. In this case, the 32-layer model uses four layers per skin depth at 23 GHz, where the difference between the two-layer and 32-layer result is 2.5%, of which a residual portion is likely due to any remaining side current. Thus, it appears that a minimum of fourlayers per skin depth should be used for the multilayer model.

The structure for Fig. 6 is an air dielectric stripline 4.3 $\mu$m thick, which is five skin depths at 10 GHz using a bulk conductivity of $3.45 \times 10^7$ S/m. The two-layer model uses $R_{\rm RF} = 3.38 \times 10^{-7}$ while the four-, eight-, 16-, and 32-layer models use $R_{\rm RF} = 0$.

Caution should be exercised whenever using any $N$-layer model. If the transmission lines are long with respect to wavelength, an odd mode (positive current on one conductor, negative current on the other) may be excited. In addition, the top/bottom split of current may need to change at discontinuities. Thus, it is recommended that all layers in an $N$-layer model be tied together with vias every quarter wavelength or so and at all significant discontinuities.

## V. One-Layer Model

The one-layer loss model uses $R_{\rm DC}$ [see (6)] corresponding to the full thickness of the conductor. However, in the skin effect region, there are actually two sheets of current. In the two-layer model, each sheet is modeled. In the one-layer model, we must combine the effect of both actual sheets of current, which are connected in parallel, into the one sheet of the model. If the current on the top and bottom sides are equal, then we simply divide $R_{\rm RF}$ by 2. However, in microstrip, this current split is not equal, as more current flows on the bottom side. In this case, $R_{\rm RF}$ is modified [2] as follows:

$$R'_{\rm RF} = R_{\rm RF}\left(k_1^2 + k_2^2\right) \tag{11}$$

where $R'_{\rm RF}$ is the equivalent single sheet $R_{\rm RF}$, $k_1$ is the fractional top-side current, and $k_2$ is the fractional bottom-side current $(k_1 + k_2 = 1.0)$. In the case of the microstrip line considered here, the two-layer model shows that the current on the bottom surface is almost 1.5 times larger than the current on the top surface. With $R_{\rm RF}$ modified as described, Fig. 7 shows the convergence compared to the 128-cell-wide 81-layer result. The 16- and 32-cell-wide and the 81-layer results are all within $\pm 0.02$ dB of each other. Analysis times range from essentially instantaneous to 4 s per frequency.

This one-layer result shows better agreement with the 81-layer model than the two-layer result. This may be due to the effect of the current on the lateral side modifying the edge singularity on the top and bottom surfaces. Fig. 8 plots the top and bottom surface current densities across the width of the line for the two- and one-layer models, all curves normalized to the current in the center of the line.

Note that both the top and bottom current of the two-layer model have a larger percentage of the total current constrained

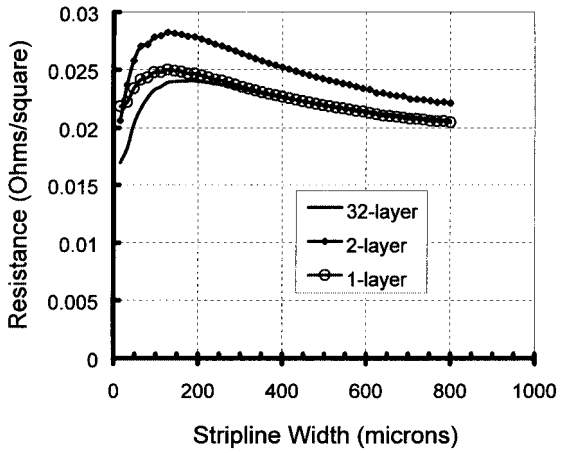


Fig. 9. Analysis of stripline resistance as a function of line width shows the effect of side current below 100 $\mu$m wide and the overestimation of resistance by the two-layer model. Stripline geometry: $t = 8.6$ $\mu$m, $\sigma = 3.45 \times 10^7, \varepsilon_r = 1.0$; ground plane spacing $= 200$ $\mu$m; frequency: 10 GHz, using $(W \times L)$ 1 $\mu$m $\times$ 5 $\mu$m cell size.

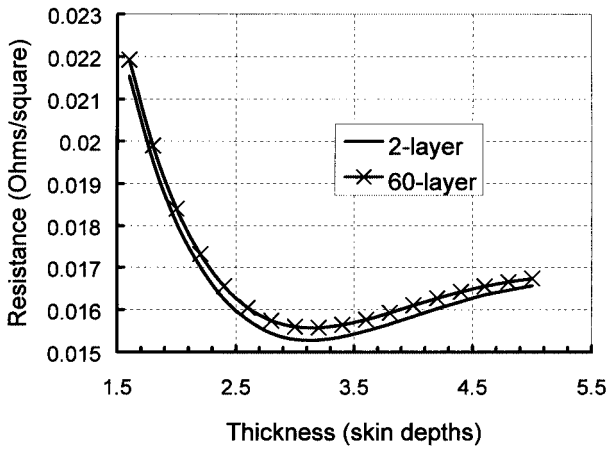


Fig. 10. Because current reverses direction at several skin depths into a conductor, there exists an optimal metal thickness for minimum loss. Stripline geometry: $w = 400$ $\mu$m, $\sigma = 3.45 \times 10^7, \varepsilon_r = 1.0$; ground plane spacing: 18.6 $\mu$m; skin depth: 0.86 $\mu$m at 10 GHz. Cell size in the two-layer model $(W \times L)$: 6.25 $\mu$m $\times$ 5 $\mu$m. Cell size in the 61-layer model: 25 $\mu$m $\times$ 20 $\mu$m.

to the edge of the conductor than the one-layer result. We suggest that this is caused by the lack of side current in the two-layer model. Consider the lossless quasi-static model of a transmission line. For the actual line, there is charge on the lateral side of the line that pushes charge out of the edge singularity onto the top and bottom surfaces. In the two-layer model, this side charge is no longer present on the side, allowing a stronger edge singularity to form, increasing the loss.

In further support of this hypothesis, Fig. 9 shows a stripline resistance as a function of stripline width. The ground plane spacing is increased to 200 $\mu$m (from the 18.6 $\mu$m of Fig. 4) so side current has an increased effect. The width of the line is swept from 16 to 200 $\mu$m. For narrow lines, we see a difference between the one- and 32-layer models. For all cases plotted, this difference is very close to the ratio of the line thickness divided by the sum of the thickness and the width (suggesting an $R_{\rm RF}$ modification to compensate for side current). Thus, we consider this difference to be due to a portion of the current flowing on the side of the line.

The two-layer model shows 15%–30% more resistance than the one-layer model. As before, this can be qualitatively explained by noting that, in the one-layer model, all the side current is on the same level. In the two-layer model, the side current is moved to either the top or bottom surface, reducing its ability to modify the edge singularity.

Note that, with the incorrect selection of $k_1$ and $k_2$, the one-layer model can be in error for loss by as much as a factor of two. While $k_1$ is always less than or equal to 0.5 in all cases so far investigated, $k_1$ can sometimes approach zero and is frequency- and geometry-dependent. Thus, if precise calculation of loss is required from the one-layer model, one should carefully evaluate $k_1$ from a two-layer analysis for the desired line geometry and frequency range in addition to considering the effect of side current. It should also be noted that the $k_1, k_2$ factors do not appear to have been previously considered in the literature.

The stripline modeled in Fig. 9 is 8.56 $\mu$m thick (ten skin depths at the 10-GHz analysis frequency) with a bulk conductivity of $3.45 \times 10^7$ S/m, subsectioned with cells 1.0 $\mu$m wide.

## VI. Minimum Loss Thickness

Fig. 10 shows the resistance of a stripline 400 $\mu$m wide. Since the width is large compared to the thickness, side current has little effect and the 61- and two-layer models yield nearly identical results. The thickness of the line is varied. Skin depth at the analysis frequency of 10 GHz is 0.8586 $\mu$m.

This plot demonstrates the counterintuitive result that, for a thickness of about three skin depths, conductor loss realizes a minimum. Both thicker and thinner conductors have greater loss. This characteristic was first proposed in [1], numerically confirmed in [12] and [13], and experimentally and numerically confirmed in [5].

That the minimum occurs at about three skin depths is concluded in [12], however, it is commented in [12] that a minimum is not seen for all microstrip line configurations. Of the few cases we considered, we did not find any for which the minimum did not occur, however, the minimum can be very slight and easily missed. Note the vertical scale of Fig. 10.

The absence of a minimum is possible because the first critical frequency [(8)] decreases as thickness increases. If the edge singularity is still emerging from the low-frequency current distribution when the line is about three skin depths thick, the minimum will be shifted and possibly eliminated.

An optimum thickness of two skin depths is proposed in [13], but only for very wide lines, and $\pi/2$ skin depths is proposed in [5]. The data presented in [1] suggest a minimum around three skin depths. We have not investigated the effect of line geometry on optimum thickness; this would be an excellent area for future research.

Convergence analyses and mesh sizes used were not reported in [12], [13], or [5]. In this paper, we have shown that an extremely small cell size is sometimes required for convergence and we consider a convergence analysis to be critical in assuring accurate results. The absence of a minimum loss thickness and the value of the optimum thickness, when observed, could be correct or it could be the result of a lack of numerical convergence.

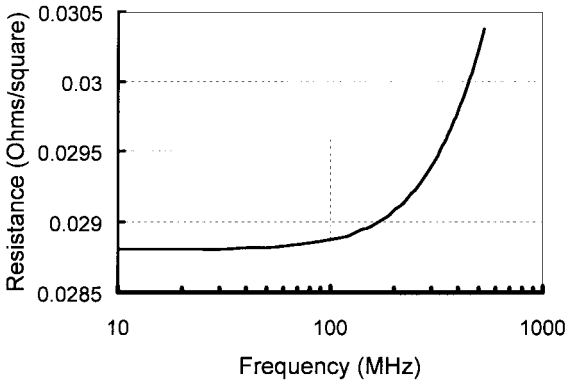


Fig. 11. Detail of the microstrip resistance of Fig. 12 near the first critical frequency of 136 MHz shows that loss starts to slowly increase as the edge singularity emerges.

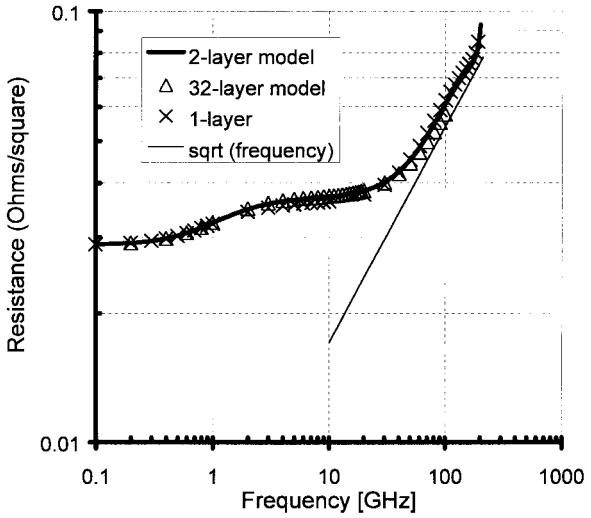


Fig. 12. Broad-band analysis of microstrip resistance shows complicated behavior as the edge singularity emerges at low frequency, and the effects of dispersion and skin effect become important at high frequency. Microstrip geometry: $w = 70\,\mu$m, $t = 1\,\mu$m, $\sigma = 3.45 \times 10^7$, $\varepsilon_r = 12.9$, $h = 100\,\mu$m. Cell size ($W \times L$): 8.75 $\mu$m $\times$ 3 $\mu$m.

The optimum thickness result is easily explained in that the skin effect current varies in both amplitude and phase as it penetrates the conductor [(2)]. In fact, at a depth of $\pi$ skin depths, the current is 180° out of phase with current at the surface. The current at that depth is actually flowing backward. This backward-flowing current increases the $I^2R$ loss while also decreasing the total current in the line. When a line is thin enough that some of this backward-flowing current is suppressed, the total loss can be less than that of a thick line.

We have simulated a hollow microstrip line similar to the line in Fig. 1 using the 81-layer model and found that, for appropriately chosen dimensions, skin effect losses are reduced by up to 20% as compared to a solid line. However, at low frequency, losses are increased by the reduction in cross-sectional area as current flows with the same phase everywhere in a given cross section.

## VII. Microstrip Loss Frequency Variation

Figs. 11 and 12 show microstrip loss as a function of frequency. This line is 70 $\mu$m wide on a 100-$\mu$m substrate with a relative dielectric constant of 12.9 and loss tangent of 0.0005. The 1.0-$\mu$m-thick metal uses a bulk conductivity of $3.45 \times 10^7$ S/m.

Fig. 11 shows low frequency loss variation detail. The first critical frequency [see (8)] is 136 MHz. The microstrip loss has indeed started a gradual increase caused by the gradual emergence of the edge singularity.

As seen in Fig. 12, the emergence of the edge singularity is complete around 3 GHz, causing the increase in loss to nearly stop. However, the loss curve still has a gradual upwards slope. This is partially due to current starting to flow preferentially on the bottom surface of the microstrip. At 1 GHz, the top and bottom currents are nearly equal. At 10 GHz, there is 4% more current on the bottom surface than on the top. At 100 GHz, the difference is 16%. The loss also gradually increases due to a gradually increasing edge singularity. This increasing preference for the current to flow on the bottom surface and outside edges also results in microstrip dispersion.

The second critical frequency [see (9)] is 29.2 GHz. Here we see the transition into square root of frequency behavior modified by the dispersion first seen in the 2–20-GHz region and by the oscillatory variation of surface impedance with decreasing skin depth.

Many of the characteristics seen here are also seen in [8, Fig. 3].

## VIII. Conclusion

The $n$-, two-, and one-layer models of microstrip loss for use in planar electromagnetic analysis are validated for high-accuracy use. The $n$-layer model, using frequency-independent surface resistance, duplicates the frequency variation of microstrip loss purely through the solution of Maxwell's equations and is validated by comparison with measurements. The two- and one-layer models, incorporating a frequency-dependent surface impedance, are validated by comparison with measurements and by comparison with the $n$-layer model. In the course of validation, it is demonstrated that the classically assumed square root of frequency behavior can be significantly modified by, for example, microstrip dispersion at high frequency and by the emergence of the edge singularity at low frequency. In addition, it is also confirmed that there is an optimum thickness for minimum microstrip loss and that current flowing on the lateral sides of a microstrip line can further influence loss. Future efforts could include quantitative analysis of the range of validity for the various models for various geometries, especially as a function of line width, and for applicability to multiple conductor transmission lines, such as coplanar waveguide and coupled microstrip lines.

## Acknowledgment

The authors would like to thank M. Ashman, A. Durham, and B. Weaver of M/A-COM for providing measured data. The authors would also like to thank the reviewers for their useful comments.

## REFERENCES


[1] R. Horton, B. Easter, and A. Gopinath, "Variation of microstrip losses with thickness of strip," *Electron. Lett.*, vol. 7, no. 17, pp. 490–491, Aug. 1971.

[2] J. C. Rautio, "An investigation of microstrip conductor loss," *IEEE Microwave Mag.*, pp. 60–67, Dec. 2000.

[3] A. E. Kennelly, F. A. Laws, and P. H. Pierce, "Experimental researches on skin effect in conductors," *Trans. AIEE*, vol. 34, pp. 1953–2018, 1915.

[4] E. Tuncer, B.-T. Lee, M. S. Islam, and D. P. Neikirk, "Quasistatic conductor loss calculations in transmission lines using a new conformal mapping technique," *IEEE Trans. Microwave Theory Tech.*, vol. 42, pp. 1807–1815, Sept. 1994.

[5] M. Konno, "Conductor loss in thin-film transmission lines," *Electronics and Communications in Japan*, pt. 2, vol. 82, no. 10, pp. 83–91, 1999. translated from *Denshi Joho Tsushin Gakkai Ronbunshi*, vol. J81-C-1, no. 8, Aug. 1998, pp. 466–473.

[6] *Sonnet User's Manual, Version 8.0*, Sonnet Software, Liverpool, NY, June 2002.

[7] A. R. Djordjevic and T. K. Sarkar, "Closed form formulas for frequency-dependent resistance and inductance per unit length of microstrip and strip transmission lines," *IEEE Trans. Microwave Theory Tech.*, vol. 42, pp. 241–248, Feb. 1994.

[8] F. Schnieder and W. Heinrich, "Model of thin-film microstrip line for circuit design," *IEEE Trans. Microwave Theory Tech.*, vol. 49, pp. 104–110, Jan. 2001.

[9] J. C. Rautio, "An ultra-high precision benchmark for validation of planar electromagnetic analyses," *IEEE Trans. Microwave Theory Tech.*, vol. 42, pp. 2046–2050, Nov. 1994.

[10] ——, "EM approach sets new speed records," *Microwaves RF Mag.*, pp. 81–96, May 2002.

[11] E. H. Lenzing and J. C. Rautio, "A model for discretization error in electromagnetic analysis of capacitors," *IEEE Trans. Microwave Theory Tech.*, vol. 46, pp. 162–166, Feb. 1998.

[12] W. Heinrich, "Full-wave analysis of conductor losses on MMIC transmission lines," *IEEE Trans. Microwave Theory Tech.*, vol. 38, pp. 1468–1472, Oct. 1990.

[13] L. P. Vakanas and A. C. Cangellaris, "A parametric study of the attenuation constant of lossy microstrip lines," *IEEE Trans. Microwave Theory Tech.*, vol. 38, pp. 1136–1139, Aug. 1990.


**James C. Rautio** (S'77–M'78–SM'91–F'00) received the B.S.E.E. degree from Cornell University, Ithaca, NY, in 1978, the M.S. degree in systems engineering from the University of Pennsylvania, Philadelphia, in 1982, and the Ph.D. degree in electrical engineering from Syracuse University, Syracuse, NY, in 1986.

From 1978 to 1986, he was with General Electric, initially with the Valley Forge Space Division, then with the Syracuse Electronics Laboratory. During this time, he developed microwave design and measurement software and designed microwave circuits on alumina and on GaAs. From 1986 to 1988, he was a Visiting Professor with Syracuse University and Cornell University. In 1988, he joined Sonnet Software, Liverpool, NY, full time, a company he had founded in 1983. In 1995, Sonnet Software was listed on the Inc. 500 list of the fastest growing privately held U.S. companies, the first microwave software company ever to be so listed. Today, Sonnet Software is the leading vendor of three-dimensional planar high-frequency electromagnetic analysis software.

Dr. Rautio was the recipient of the 2001 IEEE Microwave Theory and Techniques Society (IEEE MTT-S) Microwave Application Award.

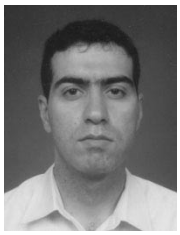

**Veysel Demir** (S'00) was born in Batman, Turkey, in 1974. He received the B.S.E.E. degree from the Middle East Technical University, Ankara, Turkey, in 1997, and is currently working toward the Ph.D. degree at Syracuse University, Syracuse, NY.

He is with Sonnet Software Inc., Liverpool, NY, as part of his research assistantship.